JOURNAL OF OPTOELECTRONICS AND ADVANCED MATERIALS Vol. 9, No. 8, August 2007, p. 2419 - 2423

Achievable qualitative parameters of optical wireless links

Z. KOLKA*, O. WILFERT, O. FISER[a]
Institute of Radio Electronics, Brno University of Technology, Purkynova 118, 612 00 Brno, Czech Republic
[a]Institute of Atmospheric Physics, Academy of Sciences of the Czech Republic, Bocni 1401, 141 31 Prague 4, Czech Republic

The estimation of optical wireless link availability is based on the synthesis of two models: the steady model of a given link and the statistical model of installation site. The steady model is based on the knowledge of link transceiver parameters from which the power budget for a given transceiver distance can be calculated. The result is the dependence of link margin on the transceiver distance. The statistical model is based on the knowledge of statistical parameters of atmosphere at a given installation site. The installation site is described by the exceedance probability of atmospheric attenuation. By means of the synthesis of both models we can obtain the estimation of link availability. In this contribution, an estimation of link availability in chosen Central - European localities is presented.

(Received May 30, 2007; accepted June 27, 2007)

Keywords: Free-space optical link, Transmission of atmosphere, Optical communication

1. Introduction

Optical wireless links (OWL) transmit data in the atmosphere by means of narrow optical beams. The availability of links spanning distances of hundreds of meters is influenced mainly by fog and low clouds. Kilometre links are influenced additionally by heavy rain and snow. The link availability depends on the link margin (steady model) and statistical parameters of the atmosphere at the link installation site (statistical model). The statistical model characterizes both the statistical properties of fade depths and the statistical properties of individual fade durations.

A systematic methodology for the design and reliability assessment of OWL has not been fully developed yet. The paper presents OWL models for reliability estimation and results of long-term measurements in selected Central-European localities.

2. Steady model of OWL

The model of optical wireless link consists of two parts: the steady model of power budget of the link and the statistical model of atmospheric transmission channel. The steady model is expressed by power balance equation (1) following from the power level diagram (Fig. 1), where $P_{m,TXA}$ is the transmitted power, α_{tot} the total attenuation between apertures RXA and TXA, and γ_{tot} the total gain of receiver [1]. The power balance equation for received power $P_{m,TXA}$ can be written as

$$P_{m,RXA} = P_{m,TXA} - \alpha_{tot} + \gamma_{tot} \text{ [dB]} \quad (1)$$

The total attenuation of the link α_{tot} is divided into: propagation attenuation α_{12} and attenuation caused by atmospheric phenomena α_{atm}. In decibels we obtain

$$\alpha_{tot} = \alpha_{12} + \alpha_{atm} \quad (2)$$

The total atmospheric attenuation α_{atm} is divided into attenuation caused by particles α_{part} and attenuation caused by turbulence α_{turb}. Assuming a homogenous stationary atmosphere, it is possible to express the attenuation caused by the particles along the path as

$$\alpha_{part} = \alpha_{1,part} L_{12} \text{ [dB]}, \quad (3)$$

where $\alpha_{1,part}$ is the attenuation coefficient [dB/km], and L_{12} is the distance between transceivers.

Using the model of a weakly turbulent atmosphere (the relative variance of optical intensity in the plane of receiver is less than 1) it is possible to express α_{turb} as [1]

$$\alpha_{turb} \approx \left| 10 \log\left(1 - \sqrt{\sigma_{r,I}^2}\right) \right| \text{ [dB]}, \quad (4)$$

where $\sigma_{r,I}^2$ is the relative variance of optical intensity in the plane of receiver given as [2]

$$\sigma_{r,I}^2 = 0.5 C_n^2 \left(\frac{2\pi}{\lambda}\right)^{7/6} L_{12}^{11/6}. \quad (5)$$

For a standard clear atmosphere ($\tilde{\alpha}_{1,part} \approx 0.5$ dB/km; $\tilde{C}_n^2 = 10^{-14}$ m$^{-2/3}$), for $\lambda = 850$ nm and for $L_{12} = 1$ km the attenuation coefficient related to turbulence is

$\tilde{\alpha}_{1,turb} \approx 2.2$ dB. The sum of both attenuations expresses the total attenuation of the clear atmosphere: $\tilde{\alpha}_{part} + \tilde{\alpha}_{turb} = \tilde{\alpha}_{atm}$.

The total gain γ_{tot} of the receiver can be divided into the geometrical gain γ_{RXA} (given by the ratio of aperture diameters D_{RXA} and D_{TXA}) and the additional gain γ_{add} (given by different distribution of optical intensity on the transmitting and the receiving aperture)

$$\gamma_{tot} = \gamma_{RXA} + \gamma_{add} = \left| 20 \log \frac{D_{RXA}}{D_{TXA}} \right| + \gamma_{add} \text{ [dB]} . \quad (6)$$

If the intensity distribution on the transmitting aperture is of the Gaussian type [3], the beam width is the same as the diameter of transmitting aperture D_{TXA} , and the intensity distribution in the receiving aperture plane is approximately constant, i.e.

$$L_{12}\varphi_t >> D_{RXA} , \quad (7)$$

the additional gain obtained will be $\gamma_{add} = 3.7$ dB. φ_t is the angle width of transmitted beam.

The propagation attenuation α_{12} and the geometrical gain γ_{RXA} can be joined into one quantity referred to as geometrical attenuation α_{geom}

$$\alpha_{geom} = \alpha_{12} - \gamma_{RXA} = \left| 20 \log \frac{D_{RXA}}{D_{TXA} + \varphi_t L_{12}} \right| \text{ [dB]}. \quad (8)$$

We can image the transmitter, atmosphere and receiver along the horizontal direction of the power level diagram (Fig. 1). The atmospheric attenuation consists of the attenuation of clear atmosphere $\tilde{\alpha}_{atm}$ and random additional attenuation α_{add}. The sum of both attenuations expresses the total attenuation of the real atmosphere $\tilde{\alpha}_{atm} + \alpha_{add} = \alpha_{atm}$.

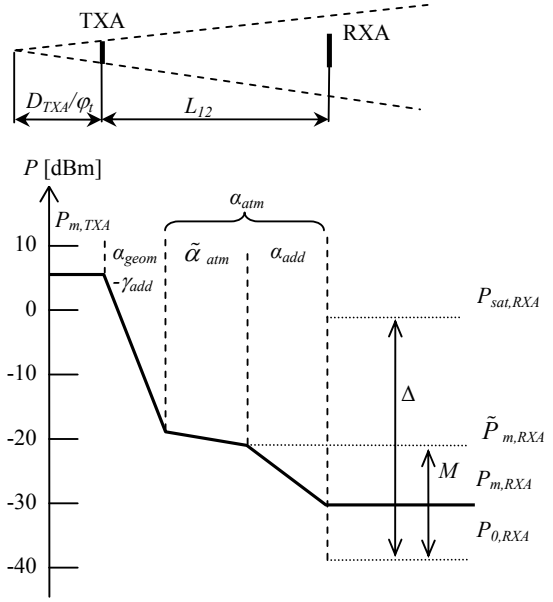

Fig. 1. Power level diagram for typical values of presented quantities.

$\tilde{P}_{m,RXA}$ is the mean power on receiving aperture RXA for the standard clear atmosphere. $P_{sat,RXA}$ and $P_{0,RXA}$ are saturation and sensitivity threshold of the receiver. Their difference gives the dynamic range Δ of receiver. The difference between received power for the clear atmosphere and the sensitivity threshold gives the link margin M. The value of M plays a crucial role in link reliability.

The maximum link range for a certain link margin M can be determined from the dependence of geometrical attenuation α_{geom} and atmospheric attenuation $\tilde{\alpha}_{atm}$ on distance L_{12}. The link margin is

$$M = \tilde{P}_{m,RXA} - P_{0,RXA} = P_{m,TXA} - P_{0,RXA} + \\ + \gamma_{add} - \alpha_{geom}(L_{12}) - \tilde{\alpha}_{atm}(L_{12}) \quad (9)$$

Considering (7) and (8), equation (9) simplifies to

$$M \doteq P_{m,TXA} - P_{0,RXA} + 20 \log \frac{D_{RXA}}{\varphi_t} - \\ - 20 \log L_{12} + \gamma_{add} - \tilde{\alpha}_{atm}(L_{12}) \quad (10)$$

The first three quantities in (10) represent the design parameters of wireless link. To have a measure for different OWL installations with respect to the atmospheric attenuation coefficient $\alpha_{1,atm}$ [dB/km] it is convenient to introduce the normalized link margin as

$$M_1 = \frac{M}{L_{12}} \text{ [dB/km]}. \quad (11)$$

The dependence of normalized link margin M_1 on L_{12} represents the steady model of OWL link. The model represents a synthesis of the power balance equation with the model of beam propagation [2] in the clear atmosphere.

3. Statistical model of installation site

A well-known disadvantage of atmospheric links is the sensitivity to meteorological factors, such as fog and precipitation, causing a significant increase of α_{add}. Fig. 2 shows a record of received optical power at RXA [4]. A fade occurs when the received optical power falls below the sensitivity threshold of the receiver, i.e. when the additional atmospheric attenuation exceeds the link margin.

With regard to the considerable difference between usual transmission rates and the processes in the atmosphere the fade durations are several orders of magnitude longer than the clock period of transmitted data.

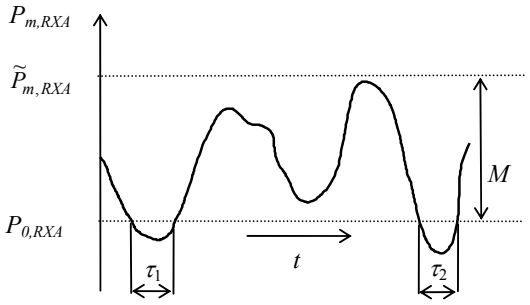

Fig. 2. Random character of received optical power for a link with fades (τ_1 and τ_2 - intervals where optical power on RXA is lower than receiver sensitivity threshold).

With respect to Fig. 2 the probability of link unavailability can be expressed as

$$P_{un} \approx \frac{T_{un}}{T} = \frac{\sum \tau_i}{T} \ , \qquad (12)$$

where τ_i are the durations of individual fades observed during a sufficiently long period T. Fig. 3 shows a six-year record of atmospheric attenuation with obvious one-year periodicity. One can see that P_{un} for various months of the year can differ significantly. To get representative figures we should use data averaged over one-year periods unless we are interested in the behavior of "seasonal" links.

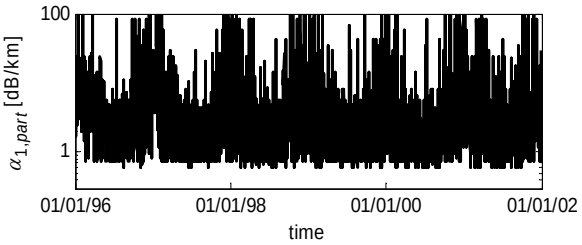

Fig. 3. Example of six-year record of $\alpha_{1,part}$.

Table 1. Monitored sites.

No	site	coordinates	altitude	period	resolution	type
1	Brno	49°09'05"N, 16°42'01"E	237 m	1996-2001	1 hour	airport
2	Namest	49°10'18"N, 16°07'08"E	452 m	1996-2001	1 hour	airport
3	Prerov	49°25'16"N, 17°24'17"E	206 m	1996-2001	1 hour	airport
4	Kopisty	50°32'40"N, 13°37'25"E	240 m	2005	15 min	town
5	Milesovka	50°33'17"N, 13°55'53"E	837 m	2005	15 min	hill
6	Liberec	50° 46' 5"N, 15° 1' 29"E	405m	2002-2005	1 hour	airport
7	Mosnov	49° 41'45"N, 18° 6' 38"E	257m	2002-2005	30 min	airport
8	Prague	50° 6' 3"N, 14° 15' 36"E	380m	1998-2005	30 min	airport
9	Karl. Vary	50°12'11"N, 12°54'54"E	606m	2002-2005	1 hour	airport

Considering the additional atmospheric attenuation $\alpha_{1,add}$ as a random variable the link unavailability can be expressed as

$$P_{un} = P(\alpha_{1,add} \geq M_1) = E_\alpha(M_1) \ , \qquad (13)$$

where M_1 is the normalized link margin (11), and E_α is the cumulative exceedance probability of additional atmospheric attenuation.

We have evaluated measurements of the meteorological visibility range from several sites, Table 1. Their local climate represents typical Central-European conditions. The data resolution ranged from 15 minutes to 1 hour. The attenuation coefficient was calculated using Kim's empirical formula [5]

$$\alpha_{1,part} = \frac{17}{V_M \left(\frac{555}{\lambda} \right)^q} \ [\text{dB/km}], \qquad (14)$$

where V_M is the meteorological visibility in km, λ is the wavelength in nm, and q depends on V_M:

$q =$ 1.6 for $V_M > 50$ km;
1.3 for 6 km $< V_M \leq 50$ km;
0.16 V_M + 0.34 for 1 km $< V_M \leq 6$ km;
$V_M - 0.5$ for 0.5 km $< V_M \leq 1$ km;
0 for $V_M \leq 0.5$ km.

According to [6] the expected accuracy of (14) is about ± 10 dB/km for a low V_M .

Fig. 5 shows empirical exceedance probability E_α for sites from Table 1. The Figure shows E_α for $\alpha_{1,atm} > 10$dB/km since lower attenuation statistics are not so important from the point of view of typical short-range links. Extreme attenuations determine the requirements on the design and installation of OWL to get acceptable link unavailability. The curves for all the sites exhibit an evident knee between 20 dB/km – 40 dB/km. The exceedance probability above the knee is roughly linear in semilogarithmic coordinates, which corresponds to an exponential-tail distribution. Table 2 summarizes the total link unavailability for the monitored sites.

Table 2. Probability of link unavailability P_{un} [%] for test sites (λ = 850nm).

M_1 [dB/km]	site				
	1	2	3	4	5
10	6.3	13	8.7	10	26
20	2.4	8.8	3.5	2.9	21
50	0.85	4.7	1.8	1.3	18
100	0.20	2.3	1.2	0.86	15

M_1 [dB/km]	site			
	6	7	8	9
10	5.6	6.5	4.1	8.0
20	1.6	1.8	2.4	3.1
50	0.50	0.80	1.0	0.81
100	0.25	0.37	0.46	0.30

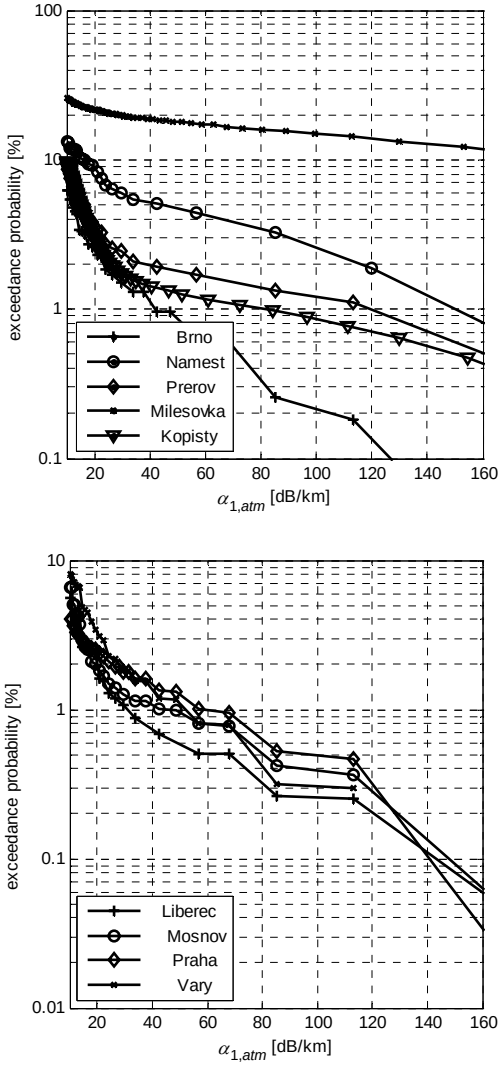

Fig. 4. Empirical cumulative exceedance probability of attenuation coefficient $\alpha_{1,atm}$, λ = 850nm.

The nomogram in Fig. 6 represents the synthesis of the steady model and the statistical model. A particular OWL transceiver is characterized by the system margin

$$M_S = P_{m,TXA} - P_{0,RXA} + 20\log\frac{D_{RXA}}{\varphi_t} \ , \qquad (15)$$

which does not depend on L_{12}. It represents the steady model of a link, which is combined with statistical parameters of the installation site, i.e. with the exceedance probability of $\alpha_{1,atm}$. The procedure for evaluating a particular installation is as follows: First, for a given system margin M_S and transceiver distance L_{12} we can find the normalized link margin M_1. The value of M_1 also represents the greatest value of additional atmospheric attenuation $\alpha_{1,add}$. Second, for a given installation site we can find the link unavailability. Fig. 5 is drawn for typical values of the system margin M_S for semiconductor laser links and for the best and the worst atmospheric conditions observed.

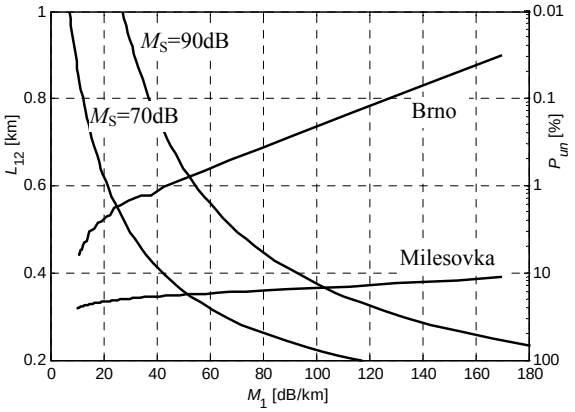

Fig. 5. Nomogram for calculation of link unavailability

If a fixed value of normalized link margin M_1 is considered, the increase of atmospheric attenuation causes fades. The fade durations form a random time series $\{\tau_i\}$ whose statistical properties are, besides unavailability P_{un}, important parameters of the optical link. It is convenient to use the conditional exceedance probability [7]

$$P(\tau \geq \tau^* \,|\, \alpha_{1,add} \geq M_1) = E_{\tau|\alpha}(\tau^* \,|\, M_1) \ , \qquad (16)$$

i.e. the probability that the fade duration is longer than τ^* in the case of a fade deeper than M_1. The cumulative exceedance probability $E_{\tau|\alpha}$ can be estimated from

$$E_{\tau|\alpha}(\tau^* \,|\, M_1) \approx \frac{n_{\tau_i \geq \tau^*}}{N} \ , \qquad (17)$$

where $n_{\tau_i \geq \tau^*}$ is the number of fades longer than τ^*, and N is the total number of fades during a sufficiently long period. The joint exceedance probability is given by

$$P(\tau \geq \tau^* \wedge \alpha_{1,add} \geq M_1) = \\ = P(\tau \geq \tau^* \mid \alpha_{1,add} \geq M_1) P(\alpha_{1,add} \geq M_1) = \\ = E_{\tau|\alpha}(\tau^* \mid M_1) E_{\alpha}(M_1) \quad . \tag{18}$$

It is the probability that at a given moment the link will be in a fade that is longer than τ^* and deeper than M_1.

The resolution of monitoring equipment allowed capturing only long-term events, i.e. fades caused by atmospheric aerosols. Fig. 6 shows the conditional exceedance probability (17) of fade durations for two selected sites. As expected, the statistics depend on the link margin chosen. Table 3 summarizes the extreme fade durations observed.

Table 3. Extreme fade durations [hour] observed at selected sites.

M_1 [dB/km]	site					
	1	3	4	5	6	8
15	47	48	33	87	49	43
30	24	35	13	86	22	41
70	15	27	12	77	11	20

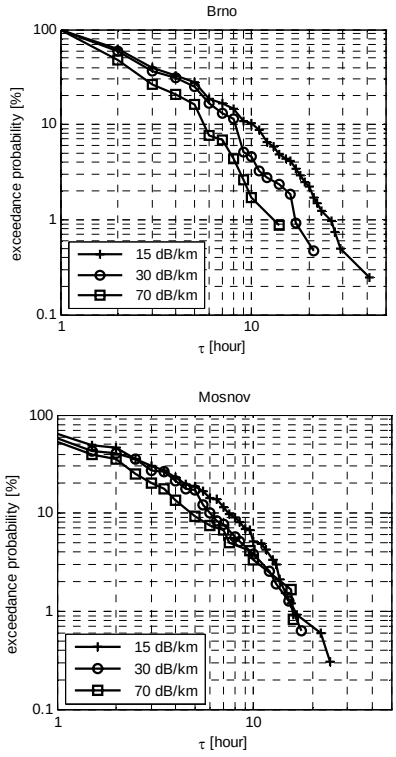

Fig. 6. Cumulative conditional exceedance probability of fade durations for different values of M_1. for sites 1 and 7.

4. Conclusion

Three models of OWL communications were presented. First, the steady model of the link, which is based on the knowledge of OWL transceiver parameters and which results in the dependence of link margin on the transceiver distance. Second, the statistical model of fades, which is based on the knowledge of statistical parameters of the attenuation coefficient $\alpha_{1,atm}$ at a given installation site and which results in the exceedance probability function of $\alpha_{1,atm}$. Third, the statistical model of fade durations, which is based on the knowledge of statistical parameters of fade durations at a given installation site.

Exceedance probabilities for some Central - European localities were presented. On the basis of the results obtained by our measurement we can conclude that present-day technology is characterized by a system margin $M_S < 90$ dB. For a link with $M_S = 90$ dB and distance $L_{12} \leq 500$ m the normalized link margin is, according to (10), $M_1 \geq 62$ dB/km. From Fig. 5 it is possible to make an estimate of the link unavailability of $P_{un} \leq 1$ % for the best installation site.

Acknowledgments

This research has been supported by the Research programs of Brno University of Technology MSM21630513, and by the Grant Agency of the Czech Republic under contracts No. 102/05/0571, No. 102/05/0732, No. 102/06/1358, and No. 102/04/2080.

References

[1] O. Wilfert, Z. Kolka, Proc. of SPIE – Vol. 5550 Free-Space Laser Communications IV, ed. Jennifer C. Ricklin, David G. Voelz, August 2004, pp. 203-213.

[2] L. C. Andrews, R. L. Phillips, C. Y. Hopen, Laser Beam Scintillation with Applications, SPIE PRESS, Washington, 2001.

[3] B. E. A. Saleh and M. C. Teich, Fundamentals of Photonics, John Wiley & Sons, New York, 1991.

[4] S. G. Lambert and W. L. Casey, Laser Communication in Space, Artech House, London, 1995.

[5] I. I. Kim, B. McArthur and E. Korevaar, Comparison of laser beam propagation at 785 nm and 1550 nm in fog and haze for optical wireless communications, Proc. of SPIE – Vol. 4214 Optical Wireless Communications III, ed. Eric J. Korevaar, February 2001, pp. 26-37.

[6] Al Naboulsi M., Sizun H., de Fornel F., Propagation of optical and infrared waves in the atmosphere, Proc. of the XXVIIIth URSI General Assembly, New Delhi, October 2005, [CD-ROM].

[7] J. Goldhirsh W. J. Vogel, Handbook of Propagation Effects for Vehicular and Personal Mobile Satellite Systems, 1998, http://www.utexas.edu/research/mopro/

*Corresponding author: kolka@feec.vutbr.cz